Gemini surfactant behavior of conventional surfactant

dodecyltrimethylammonium bromide with anionic azo dye Sunset Yellow in

aqueous solutions

Erol Akpinar^{1*}, Nazli Uygur¹, Gokhan Topcu¹, Oleg D. Lavrentovich², Antônio Martins
Figueiredo Neto³

¹ Bolu Abant Izzet Baysal University, Faculty of Arts and Sciences, Department of Chemistry, 14030, Golkoy, Bolu, Turkey

² Advanced Materials and Liquid Crystal Institute, Materials Science Graduate Program and Department of Physics, Kent State University, Kent, OH, USA

³ Universidade de São Paulo, Instituto de Fisica, Rua do Matao, No. 1371, 05508-090, São Paulo, SP, Brazil

Abstract

In this study, the interaction of an anionic azo dye Sunset Yellow with conventional cationic surfactant dodecyltrimethylammonium bromide (DTMABr) has been examined as a function of the dye concentration at 25°C by electrical conductivity and UV-VIS spectroscopy measurements. Carpena's method, combined with Aguiar's approach, was applied to the analysis of the conductivity data for evaluating the micellization parameters such as critical micelle concentrations (cmc), degree of counterion bindings (β), and micellization Gibbs free energies ($\Delta_{mic}G$) from the specific conductivity-surfactant concentration curves. The UV-VIS absorption spectroscopy measurements were performed to obtain information on the dye concentration dependence of the stacking properties of Sunset Yellow in water. The results indicated that although DTMABr is a conventional surfactant with a single alkyl chain, it shows gemini surfactant behavior at relatively high dye concentrations.

Keywords: Surfactant-dye interactions, micellization parameters, Carpena's method, Aguiar's

approach, conventional surfactant, gemini surfactant behavior, electrical conductivity, UV-VIS

spectroscopy.

Author for correspondence: Dr. Erol Akpinar; e-mail:akpinar e@ibu.edu.tr

1. Introduction

Surfactant/dye interactions are important due to their applications in industry such as

textile, photography, cosmetics, food, pharmaceutical [1-5]. In the mixtures of surfactants/dyes,

the nature and the strength of the interactions between surfactants and dyes play a key role for

their applications [6]. From this respect, the suitable surfactant/dye systems are chosen and

investigated by several methods such as conductivity, UV-VIS spectroscopy, surface

tensiometry, potansiometry, fluorescence [6-11]. In those mixtures, either conventional single-

chain or gemini surfactants have been used. It was reported that the latter ones exhibit superior

features with respect to the former one in some applications [11].

In the case of the oppositely charged surfactant/dye systems, some parameters affect the

interactions surfactants between the and dyes [4,12-17]. Especially, the

electrostatic/hydrophobic interactions between ionic surfactant and dye species [10,18], their

chemical structures [19,20], and pH [6,21] are crucial for the formation of surfactant/dye

aggregates. As it is expected, because the gemini surfactants have higher charge density on their

head groups, they produce a stronger electrostatic interaction with oppositely charged dye

molecules with respect to the conventional single-chain surfactants [4,11].

The surfactant-dye interactions are important not only in diluted aqueous micellar

solution of the surfactant/dye but also in lyotropic liquid crystals. In recent studies [22,23], it

was observed that those interactions are responsible for the formation of different lyotropic

structures, especially nematic ones. Those studies showed for the first time that the

2

chaotropic/kosmotropic property of dye molecules plays crucial role in micellar systems because this property determines the formation of the ion pairs/complexes in the pre-micellar and binding the dye molecules to the micelle surfaces in the post-micellar regions.

Some azo dyes were used to investigate surfactant-dye interactions due to their important applications as organic colorants [5,11]. Most common ones are tartrazine [24,25], Sunset Yellow [6,11,17,26], amaranth [17,27], methyl orange [28,29], crystal violet [29,30], congo red [31] etc. It was reported that azo dyes may form dye-surfactant complexes (D_xS_y) in aqueous submicellar solutions [28,31,32]. The formation of D_xS_y complexes may be well characterized from spectral shifts in the maximum absorption values by UV/Vis spectroscopy [33]. In these complexes, association of dye with the surfactant molecule depends on the surfactant alkyl chain length. For instance, the surfactant alkyl chains consist of eight to twelve (thirteen to eighteen) -CH₂ groups, the complexes are formed by one (two) surfactant(s) per dye, i.e. DS (DS₂) complexes [32,34]. Furthermore, the extent of the interactions between ionic groups of dyes and surfactant ionic head groups are also important in the formation of dyesurfactant associations in the micellar solutions [23,31]. The characteristics of these interactions determine the organization of dye-surfactant complexes or ion pairs in the solutions as Haggregations (face-to-face stacking or sandwich-type arrangement) or J-aggregations (head-totail stacking or slipped arrangement) [35,36,37,38]. Because the dyes have chromophore groups, the role of the interactions between dyes and surfactants on the formation of the aggregations can be seen in the loss of the absorbance of the chromophore groups [11,39,40] and the shift of λ_{max} [24]. While the former one is the evidence of the surfactant-dye interactions, the latter one is related to the type of the aggregations. A bathochromic (towards the or "red") shift towards longer wavelength with respect to the λ_{max} of the monomer dye in the absorbance spectra shows the presence of J-aggregates in surfactant-dye solutions [41]. Inversely, a hypsochromic or blue shift towards a shorter wavelength is an evidence of the existence of H- aggregates in those solutions [41]. Thus, by analyzing the absorption spectra of dye solutions in the presence of the surfactants, how the surfactants encourage the dye aggregations is determined.

The surfactant-dye interactions were, in general, examined at very dilute dye concentrations in several studies. In the present study, we examined the surfactant-dye interactions at low and relatively high Sunset Yellow concentrations in DTMABr/water solutions. Some studies were reported for investigating the interaction of Sunset Yellow with cationic surfactants at constant low Sunset Yellow concentrations but, to the best of our knowledge, not at high concentrations. Electrical conductivity results showed that while Sunset Yellow exhibited similar interaction properties with a conventional single—chain DTMABr surfactant as reported in the literature, however, at high dye concentrations DTMABr-Sunset Yellow solutions exhibit gemini-surfactant behaviour. Furthermore, UV-VIS absorbance measurements indicate that, at low (high) Sunset Yellow concentrations, the formation of Haggregates (J-aggregates) are dominant-prevalent in the dye solutions than as compared to J-aggregates (H-aggregates) in the absence of the surfactant.

2. Experimental

DTMABr, dodecyltrimethylammonium chloride (DTMACl), dodecyldimethylammonium bromide (DDMEABr), tetradecyltrimethylammonium bromide (TTMABr), hexadecyltrimethylammonium bromide (HTMABr) and sodium dodecylsulfate (SDS) were purchased from Sigma and Merck in high purities (>98-99%). Potassium laurate (KL) was synthesized from the neutralization of lauric acid with potassium hydroxide, KOH, as described in Refs. [42,43]. Sunsey Yellow (SSY) was also commercially available from Sigma with dye content of 90%. Because the purity of SSY is important for obtaining reliable and reproducible results, it was purified three times considering the procedure

given in [44,45]. Ultrapure water was provided by Millipore Direct-Q3 UV, which produces a water having 18.2 M Ω .cm of resistivity at 25°C, for the preparation of isotropic micellar solutions.

Electrical conductivity measurements were performed in a Mettler Toledo S470 SevenExcellence conductivity meter at 25.0°C to determine micellization parameters, critical micelle concentrations (cmc), degree of counterion bindings to the micelles (β), and micellization Gibbs free energies ($\Delta_{mic}G$). The dip-type conductivity cell was placed in a handmade metallic (made from Al) sample holder in which water was circulated for providing stable temperature by the water circulating bath (Polyscience SD07R). The cell constant was read as 0.549231 cm⁻¹ in the instrument and verified by using 0.1 M, 0.01 M and 0.001 M KCl solutions. The conductivities were measured as a function of the surfactant concentration by the successive addition of stock solutions of surfactants into the cell including ultrapure water and SSY/water solutions, separately. The stock solutions were added by 10 µL of micropipette (Eppendorf). To keep the water loss at the minimum level, the conductivity cell was closed well, except during the addition of the stock solution. For each surfactant/water surfactant/SSY/water solutions, the conductivities were measured at ~50 different total surfactant concentrations until reaching the concentration of the surfactant to about 2-2.5 times of the critical micelle concentrations. The measurements were repeated at least three times for each concentration by keeping the error <5%.

A Spectrum SP-UV 500VDB double beam spectrophotometer (Perkin Elmer Co.) was used for recording the UV/VIS absorption spectra of the Sunset Yellow/water and the surfactant/Sunset Yellow/water mixtures. The absorption spectra in the range of 300-700 nm with a 0.5 nm wavelength resolution were recorded using a pair of quartz cuvettes of 1.0 cm optical path. The quartz cuvettes including water and the solutions were kept on the reference side and the sample side, respectively. Both cuvettes were placed in the thermostated cell

compartments at 25°C. Surfactant-dye solutions were prepared by dissolution of DTMABr at the concentrations below and above its critical micelle concentration (0.00 mmol/kg-35.7 mmol/kg) in the SSY/water solutions. SSY/water solutions were prepared at different SSY concentrations in the range of 0.04-2.21 mmol/kg. Similar to the electrical conductivity measurements, the UV-VIS absorbance measurements were carried out at 25°C. Each measurement was repeated at least three times and the error in the measurements was <5-6%.

3. Results and Discussions

3.1. Method to determine the critical micelle concentrations of the surfactants

The cmc of the surfactant molecules is determined with different methods. The most common one is the measurement of the conductivity (κ) of the surfactant solutions as a function of the surfactant total concentration (C). Two different regions are observed in the κ -C graphs: the pre-micellar region below the cmc and the post-micellar region above the cmc. In both regions, the κ -C curves are linear with the slopes of S_1 and S_2 , respectively, and the degree of counterion dissociation (α = S_2/S_1) and then the degree of counterion binding (β =1- α) are evaluated. When the transition occurs from the pre-micellar region to the post-micellar region, the change in the κ -C may be abrupt or gradual. As a conventional way (Williams's method [46]), the cmc can be determined from the intersection of two linear curves obtained in the pre-and post-micellar regions, separately. Although this way can give the cmc values with small and acceptable uncertainties if the transition is abrupt, the gradual transition causes high uncertainties in the cmc values [47]. For the latter case, an alternative way was proposed by Carpena et. al [48] and applied to some surfactant solutions in the literature [49,50,51,52]. The first derivative of the κ -C curves gives a Boltzmann type sigmoid according to the following equation

$$\kappa = \frac{A_1 - A_2}{1 + e^{(C - C_0)/\Delta C}} + A_2 \tag{1}$$

where the parameters C_0 , and A_1 and A_2 are the center of the width of the transition (ΔC), and slopes of the pre-micellar and post-micellar straight lines, respectively. Carpena's method proposes that if the first derivative of the κ -C curve of the experimental raw data is fitted to the Eq. 1 to obtain the parameters, then, because the raw data need to behave as the integral of the sigmoid (Eq. 2), the fitted conductivity data as a function of the surfactant concentration are determined from

$$\kappa = \kappa_0 + A_1 C + \Delta C (A_2 - A_1) \ln \left(\frac{1 + e^{(C - C_0)/\Delta C}}{1 + e^{-C_0/\Delta C}} \right)$$
(2)

The cmc value is precisely evaluated from the first derivative of the fitted data after the integration [47]. Furthermore, the degree of counterion dissociation is calculated from the ratio of A_2/A_1 . For example, the experimental raw data and it's non-fitted first derivative for SDS/water are given in Figure 1a, and their fitted curves are plotted in Figure 1b considering Carpena's method (Eq. 2) for the comparison.

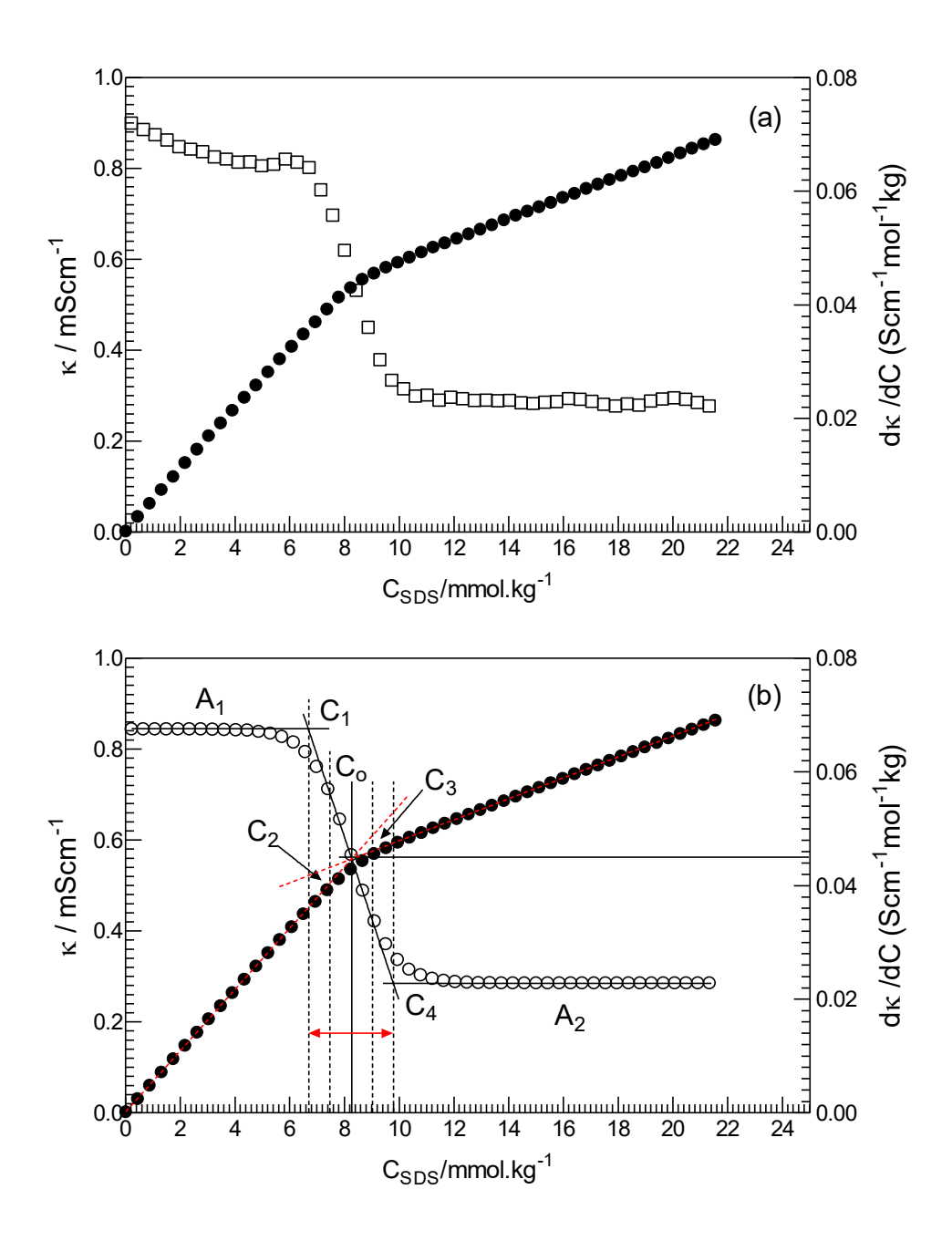


Figure 1. (a) Conductivity versus total surfactant concentration (κ-C) curve of experimental raw data (•) and it's non-fitted first derivative, dκ/dC, (\Box) for SDS/water solution at 25.0°C. (b) Same curves obtained from their fitted curves, (•) for κ-C and (\circ) for dκ/dC. The two-headed red arrow shows total concentration distance (4 Δ C) and it consists of four equal regions separated by vertical dashed lines, each of which corresponds to the concentration distance Δ C.

In 2003, Aguiar et. al. considered a wayan approach, which supports Carpena's method, to solve the problem on of the precise determination of the cmcs of surfactants when the transition from pre-micellar region to the post-micellar one is gradual [53]. Their study was

based on the pyrene 1:3 ratio method. In this method, the pyrene 1:3 ratio decreases as a function of the surfactant concentration by giving a typical sigmoidal curve (Eq. 1) similar to the one in the Figure 1b. According to their treatments, the slope of the tangent line at the center of the sigmoid is

$$\left[\frac{d(I_1/I_3)}{dC}\right]_{C=C_0} = \frac{A_2 - A_1}{4\Delta C}$$
 (3)

where C₀ still corresponds to the center of the sigmoid. After reorganization and simplifying some terms in the equations given in the Ref. [53], the authors showed that there exists a second cmc at $C_0 + 2\Delta C$. Our results are in good agreement with Aguiar's approach. In Figure 1b, the tangent line intersects with A₁ and A₂ at the concentrations C₁ and C₄, respectively. The concentration distance between C1 and C4 corresponds to 4 Δ C. Each part bordered by the dashed vertical lines before and after the center of the sigmoid (C_0) is equal to the ΔC . Until reaching to the C₁, the conductivity of the solution increases linearly as the concentration of the solution increases with a constant slope. From C_1 to C_2 ($\approx C_1 + \Delta C$), the curve starts to be gradual, i.e. the transition from monomer state of the surfactant to the micellar state begins. Further increase in the concentration from C_2 to C_0 ($\approx C_2 + \Delta C$) causes the curve to be more gradual. This can be seen from the deviation of the red-dashed straight line of the κ-C data. Opposite situation is observed from C_0 to C_3 ($\approx C_0 + \Delta C$) and from C_3 to C_4 ($\approx C_3 + \Delta C$). Especially, the transition at the concentration C₄ is important for discussing our results because it is equal to $C_0 + 2\Delta C$ as predicted by Aguiar et al. After the point C_4 , the increase in the concentration of the surfactant leads to linear increase in the conductivity with another constant slope, which is smaller than the one obtained before C₁. In other words, the micellization is completed and the solution consists of stable micelles within the working concentration range. For other selected ionic surfactants (KL, DDMEABr, DTMACl, DTMABr, TTMABr and HDTMABr), the similar κ -C curves were obtained, Figure 2. Their micellization parameters

are given in Table 1 and 2. The micellization Gibbs energies were calculated from the following equation [54]:

$$\Delta_{\text{mic}}G = (1+\beta)RT \ln X_{\text{cmc}} \tag{4}$$

where R is ideal gas constant (8.3145 J K^{-1} mol⁻¹), T is absolute temperature (K) and X_{cmc} is mole fraction of the surfactant at cmc.

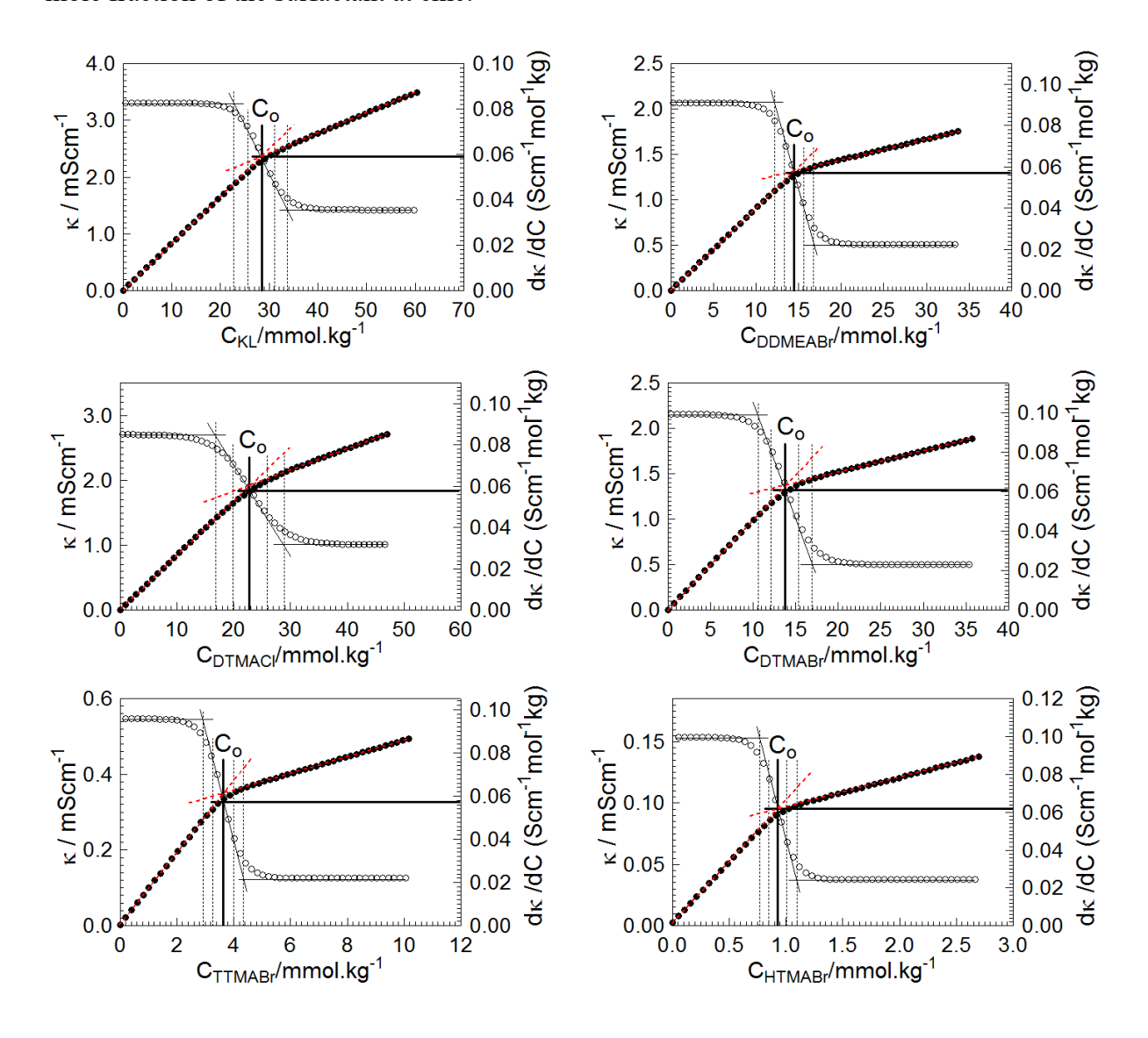


Figure 2. Conductivity versus total surfactant concentration (●) and their first derivative (○) graphs for the surfactants, considering Carpena's method and Aguiar's approach.

Table 1. Critical micelle concentrations of the surfactant molecules at 25°C, obtained from the conventional method, Boltzmann sigmoidal, and Carpena's method with Aguiar's approach. All concentrations are in mmol.kg⁻¹. The values in the parantheses are from the literature.

Surfactant	Conventional method	Boltzmann sigmoidal (differentiation)					Carpena's method (integration)						
	CMC	ΔC	\mathbf{C}_1	C_2	Co	C_3	C ₄	ΔC	C_1	C_2	Co	C_3	C ₄
SDS	8.30 (7.68- 8.56 ^{a-g,i})	0.73 (0.28 ^h)	6.81	7.53 (7.62 ^h)	8.26 (8.22 ^h ,8.29 ⁱ)	8.99	9.71	0.78	6.70	7.48	8.26 (8.28 ⁱ)	9.03	9.81
KL	28.39 (27.2 ^j)	2.65	23.04	25.69	28.34	30.98	33.63	2.71	22.91	25.63	28.34	31.05	33.76
DDMEABr	14.50 (14.0- 15.2 ^{k-m})	1.05	12.37	13.43	14.48	15.53	16.59	1.15	12.19	13.33	14.48	15.63	16.77
DTMACl	22.86 (20.3- 22.60 ^{d,k,n-p})	2.98	16.84	19.82	22.81	25.79	28.77	3.01	16.78	19.79	22.81	25.82	28.83
DTMABr	13.84 (13.50- 16.0 ^{a,q-t})	1.95 (0.77 ^h)	10.24	12.19	14.14 (13.60 ^h)	16.09	18.04	2.09 (1.21 ^u)	9.91	12.00	14.08 (15.6 ^u)	16.18	18.27
TTMABr	3.67 (3.60- 3.78 ^{i,s,t,v,w})	0.32 (0.21 ^h)	2.99	3.31	3.63 (3.73 ⁱ)	3.95	4.27	0.35 (0.138 ^u)	2.93	3.28	3.63 (3.75 ⁱ)	3.98	4.33
HTMABr	0.931 (0.92- 1.00 ^{a,i,w,y})	0.064 (0.057 ^h)	0.799	0.863	0.928 (0.96 ⁱ)	0.992	1.06	0.079 (0.121 ^u)	0.770	0.848	0.927 (0.97 ⁱ)	1.01	1.08

^a [55], ^b [56], ^c [57], ^d [58], ^e [29], ^f [59], ^g [30], ^h [53], ⁱ [48], ^j [60], ^k [61], ¹ [62], ^m [63], ⁿ [64], ^o [65], ^p [66], ^q [67], ^r [11], ^s [68], ^t [69], ^u [70], ^v [71], ^w [72], ^y [73].

Table 2. Degrees of counterion dissociation and binding, and micellization Gibbs free energy of the surfactant molecules at 25°C, evaluated from the cmc values given in Table 1. The values in the parantheses parentheses are from the literature.

	(l method	Boltzmar	dal (differentiation)	Carpena's method (integration)				
Surfactant	α	β	−∆ _{mic} G°/ kJ.mol ⁻¹	α	β	-Δ _{mic} G°/ kJ.mol ⁻¹	α	β	-Δ _{mic} G°/ kJ.mol ⁻¹
SDS	0.344 (0.369 ^a)	0.656 (0.62 ^b)	36.13 (35.46 ^b)	0.351 (0.369 ^a)	0.649	36.02	0.334 (0.368 ^a)	0.666	36.37
KL	0.435	0.565	29.38	0.424	0.576	29.60	0.423	0.577	29.62
DDMEABr	0.254 (0.261°)	0.746	35.68 (35.60°)	0.249	0.751	35.80	0.247	0.753	35.83
DTMACl	0.390 (0.389°)	0.610	31.15 (30.56 ^d , 31.43 ^e)	0.366	0.634	31.56	0.366	0.634	31.57
DTMABr	0.242 (0.244- 0.281 ^{a,e-h})	0.758 (0.75- 0.756 ^{e,h})	36.19 (34.81- 36.0 ^{e,g,h})	0.232 (0.251 ^a)	0.768	36.39	0.229 (0.248 ^a)	0.771 (0.75 ⁱ)	36.33 (35.48 ⁱ)
TTMABr	0.235 (0.227, 0.23 ^{a,j})	0.765 (0.77 ^j)	42.10 (42.10, 42.30 ^{j,k})	0.229 (0.231 ^a)	0.771	42.27	0.228 (0.230 ^a)	0.772 (0.76 ⁱ)	42.3 (41.83 ⁱ)
HTMABr	0.255 (0.243 ^a)	0.745 (0.77 ^b)	47.50 (46.45- 48.30 ^{b,k,l})	0.251 (0.250^{a})	0.749	47.66	0.248 (0.241 ^a)	0.752 (0.76 ⁱ)	47.76 (47.86 ⁱ , 48.1 ^l)

^a [48], ^b [56], ^c [61], ^d [66], ^e [74], ^f [63], ^g [75], ^h [75], ⁱ [70], ^j [76], ^k [71], ^l [49].

Tables 1 and 2 show the micellization parameters (cmc, α , β and $\Delta_{mic}G$) for the surfactants at 25.0 °C, obtained from three different ways. The results are in good agreement with the literature values. Furthermore, Carpena's method, considering together with Aguiar's approach, seems us to be more applicable way to DTMABr/SSY solutions because they exhibited the gradual transitions from the pre-micellar to the post-micellar region. By this way, we evaluated the micellization parameters of DTMABr/SSY solutions with lower uncertainties and investigated the DTMABr-SSY interactions at different SSY concentrations in the following part.

3.2 Behavior of micellar solutions of DTMABr with SSY

Sunset Yellow (disodium 6-hydroxy-5-[(4-sulfophenyl)azo]-2-naphthalenesulfonate) has an aromatic part and two ionic –SO₃⁻ moieties bound to the end regions of this part, Figure 3. It is a 1:2 type electrolyte and it ionizes in water to give one SSY²⁻ anion and two Na⁺ cations per unit formula. It was proved that the SSY molecule is in hydrazone form rather than azo form in aqueous medium [77]. The hydrogen bond in the hydrazone form provides it to exhibit a stable planar structure [41].

Figure 3. The tautomeric forms of the Sunset yellow molecule [41].

Before discussing the results of DTMABr-SSY solutions, it would be useful to mention some studies given in the literature. Shahir et al. [24] investigated the properties of

surfactant/dye solutions composed of an anionic azo dye tartrazine, like Sunset Yellow, and single chain conventional surfactant and gemini surfactants by electrical conductivity. The conventional surfactant was TTMABr, and gemini surfactants were N,N'-ditetradecyl-N,N,N',N'-tetramethyl-N,N'-butanediyl-diammonium dibromide (14,4,14) and N,N'didodecyl-N,N,N',N'-tetramethyl-N,N'-butanediyl-diammonium dibromide (12,4,12). If tartrazine-added solution is compared with tartrazine-free TTMABr/water solution, the cmc of TTMABr decreased slightly from 3.67 mM to 3.60 mM and in both cases the conductivity of the solutions increased linearly from starting point to the cmc of TTMABr. However, in the case of presence of the gemini surfactants, the conductivity of the solutions increased slightly at very low surfactant concentrations, then increased more sharply and linearly until reaching the cmcs of the gemini surfactants. Furthermore, the transition from monomer state to micellar state turned into more gradual by giving two more break points on the conductivity-surfactant concentration curve. In another study, Fazeli et al. [11] examined the surfactant-dye interactions in the DTMAB/SSY solutions at a fixed SSY concentration (0.04 mM) via surface tension, UV-VIS spectroscopy and zeta potential measurements, but not via electrical conductivity. They reported the decrease in the cmc of DTMABr from 14.85 mM to 8.46 mM by the addition of SSY to the solution. However, Nazar and Murteza [6] stated that the presence of SSY (0.044 mM) changed the cmc of HTMABr from 0.9 mM to 1.18 mM, although the concentration of SSY was greater than in Fazeli et al. study [11]. In addition, it was shown that addition of another azo dye, methyl orange (1.01 mM), slightly increased the cmcs of DTMABr, SDS and TX-114 surfactants from 14.43 mM, 8.00 mM and 0.24 mM to 14.48 mM, 8.11 mM and 0.25 mM, respectively [29]. It is seen that the addition of methyl orange slightly changed the cmcs of the surfactants. The similar situation was also reported for cetyltrimethylammonium bromide/reactive red 223 mixtures [78]. Summarily, in general, for low dye concentrations, the cmcs of surfactants slightly change or remain unchanged in the presence of dye molecules.

Figure 4 shows total DTMABr concentration-dependence of specific conductivity of the DTMABr/SSY/water solutions at different SSY concentrations. As it can be seen, except 0.04 mmol/kg SSY concentration, the behavior of the curves is similar to that of gemini surfactant/tartrazine solutions [24] at low DTMABr concentrations, and as the concentration of SSY increases this behavior is more dominant (Figure 4). The region, bordered by red-dashed line rectangular in the Figure 4, was investigated more precisely (Figure 5). As the concentration of the DTMABr concentration increases there are two more break points on the curve, which was labelled as concentrations C_p and C_C, respectively, in this study. The attributed formation Jappearance of these points was to the of aggregation/precipitation/redissolution process as reported for TTMABr/tartrazine solutions [24]. It means that DTMABr causes the formation of H-aggregation of SSY molecules at 0.04 mmol/kg SSY concentration, as reported for this concentration of SSY in the literature [11], and it encourages the J-aggregation of SSY at the SSY concentrations ≥ 0.168 mmol/kg. Figure 6a shows the SSY concentration dependence of the concentration C_C, and it can be seen that as the concentration of the SSY increases the formation of the J-aggregates is more favored.

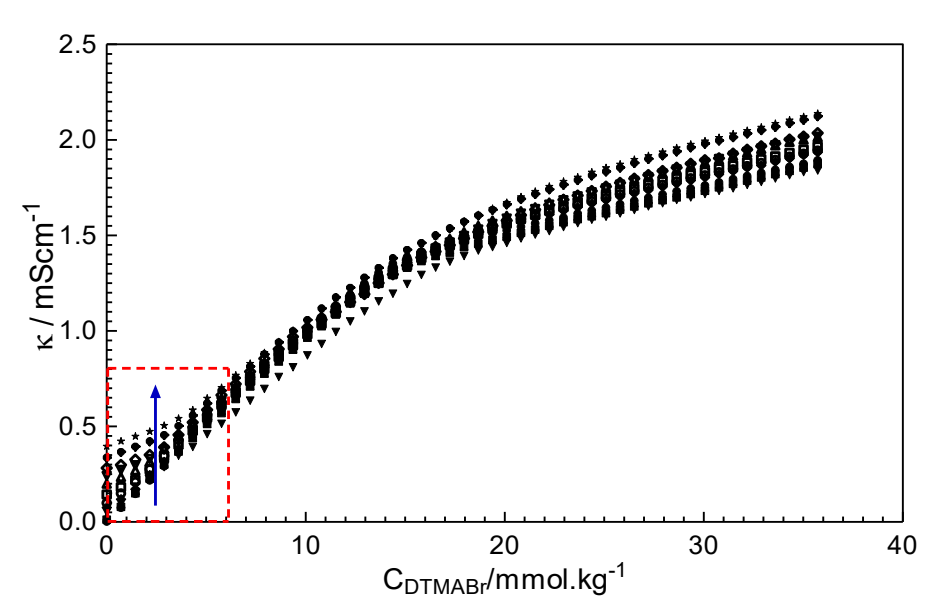


Figure 4. DTMABr concentration dependence of specific conductivity at different SSY concentrations (0.04-2.21 mmol/kg). Blue arrow shows the direction along which the SSY concentration increases in the solutions. Within the region bordered by the red-dashed line rectangular, the gemini surfactant behavior in the presence of dye was observed.

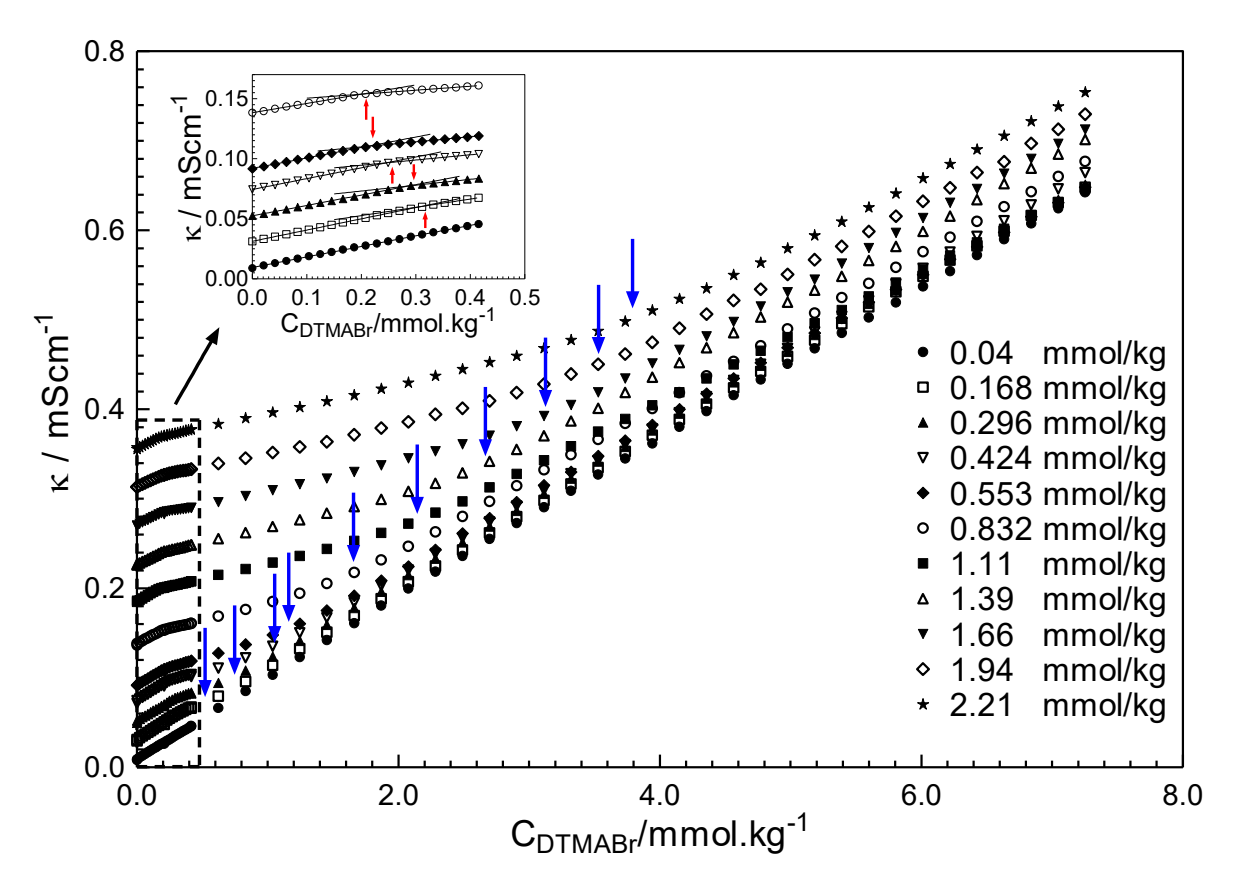


Figure 5. Specific conductivity versus DTMABr concentrations at different SSY concentrations (4.00-2.21 mmol/kg). The blue arrows correspond C_C values. (Inset) The red arrows show C_p concentrations between 0.04-0.832 mmol/kg SSY. The SSY concentrations greater than 0.832 mmol/kg gives similar specific conductivity curves and C_p values with 0.832 mmol/kg SSY.

Some dye molecules may spontaneously aggregate, depending of dye concentrations, to form stacks as dimers, trimers, tetramers,... in aqueous solutions [24,31,79,80]. The formation of dye stacks affects polar environment around chromophore groups and this situation causes the change in the UV/VIS absorption spectra of dye-surfactant solutions. To clarify whether dye stacking affects gemini surfactant behavior (Figures 4 and 5) of DTMABr-SSY solutions, UV/VIS absorption spectra (Figures 6 and 7) and conductivity (Figure 8a) of SSY solutions as a function of SSY concentration in the absence of DTMABr were studied. In other words, before discussing the interactions between DTMABr and SSY, it would be better if we examine the interactions between SSY molecules in the absence of DTMABr in the solutions to understand whether the SSY-stacking plays a role on gemini surfactant behavior of DTMABr

in the presence of SSY. Figures 6 and 7 show the spectral changes observed at low and relatively higher SSY concentrations in the absence of DTMABr. Figure 6 exhibits UV-VIS spectra of dye solutions at dilute SSY concentrations. Until ~0.10 mmol/kg SSY- concentration, the dye solutions obey Beer-Lambert's law, exhibiting linear change with SSY concentrations, however, deviations were observed > 0.10 mmol/kg (Figure 8b). These deviations arise from interactions between the absorbing species (i.e. chromophore groups of SSY) and to alterations of the refractive index of the medium. It is known that if dye molecules are present in the solution as monomers and no interaction occurs between them, the solution obeys the law, i.e. dyes molecules do not self-aggregate due to the repulsive forces between the similarly charged parts of the dye molecules. Conversely, deviations from the law are observed if dye molecules interact one with another, which results in the dye stacking. Thus, the deviations observed for SSY-concentrations greater than 0.10 mmol/kg (in the absence of DTMABr, Figure 8b) are attributed to the SSY-stacking as a result of π - π attractive interactions between dye molecules, which dominates the electrostatic repulsions between negatively charged $-SO_3^-$ groups of SSY molecules.

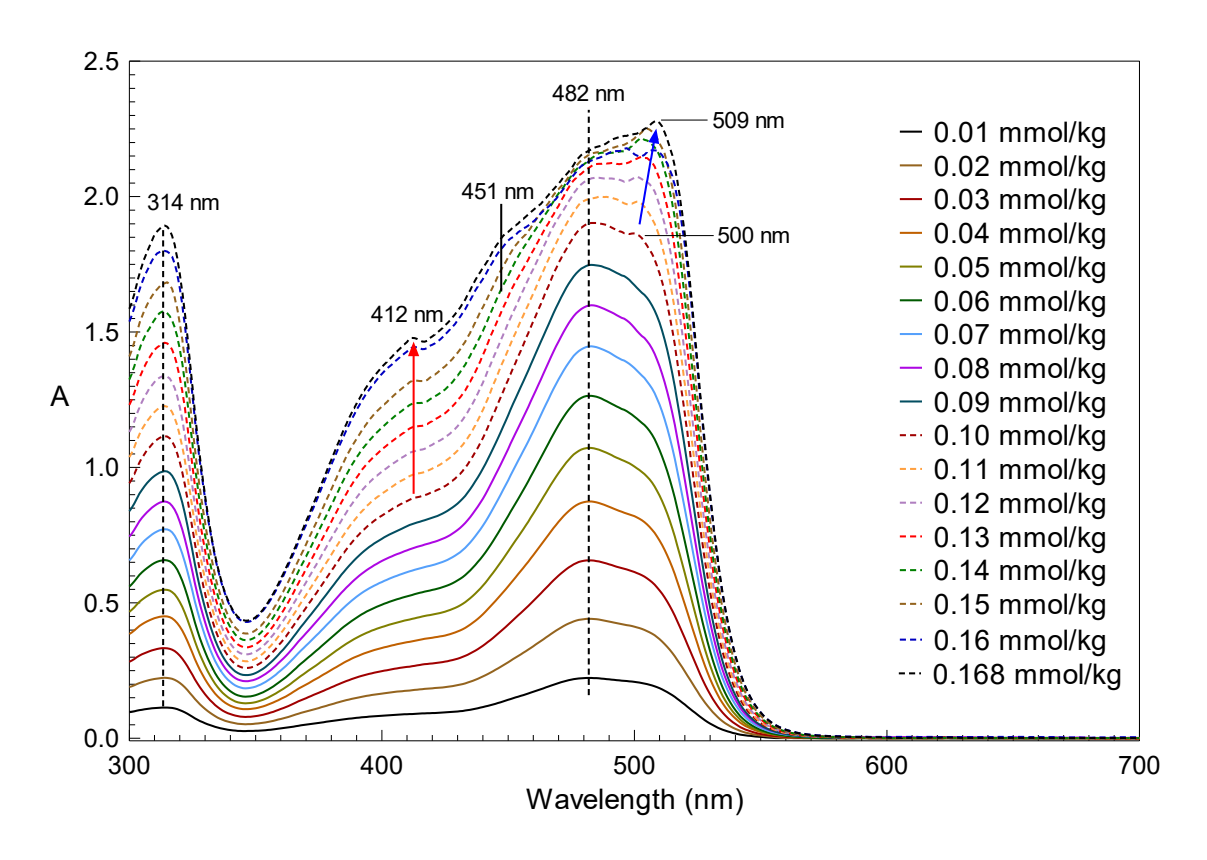


Figure 6. UV/VIS absorption spectra of SSY/water solutions varying the SSY concentrations between 0.01 - 0.168 mmol/kg in the absence of surfactant at 25°C.

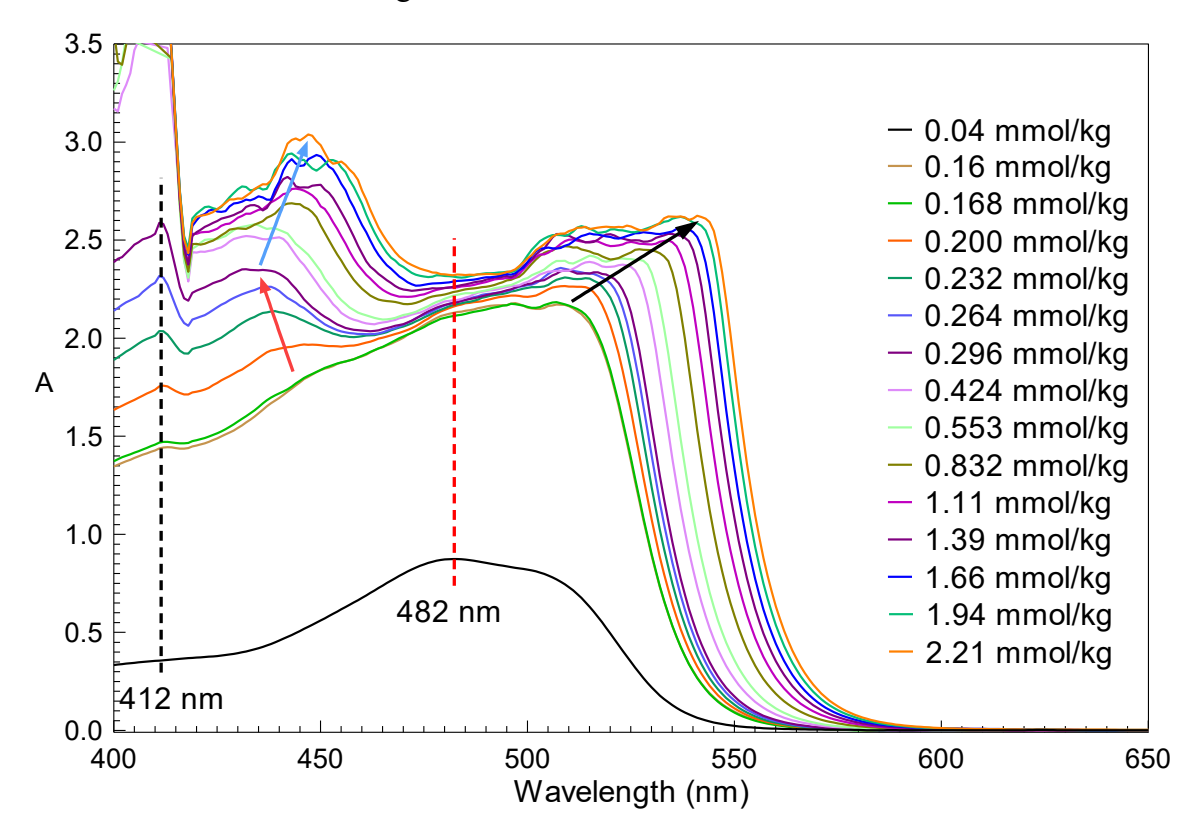


Figure 7. UV/VIS absorption spectra of SSY/water solutions varying the SSY concentrations between 0.200 - 2.21 mmol/kg in the absence of surfactant at 25°C. The sepctra for 0.04, 0.16 and 0.168 mmol/kg SSY concentrations are given in this figure for comparison.

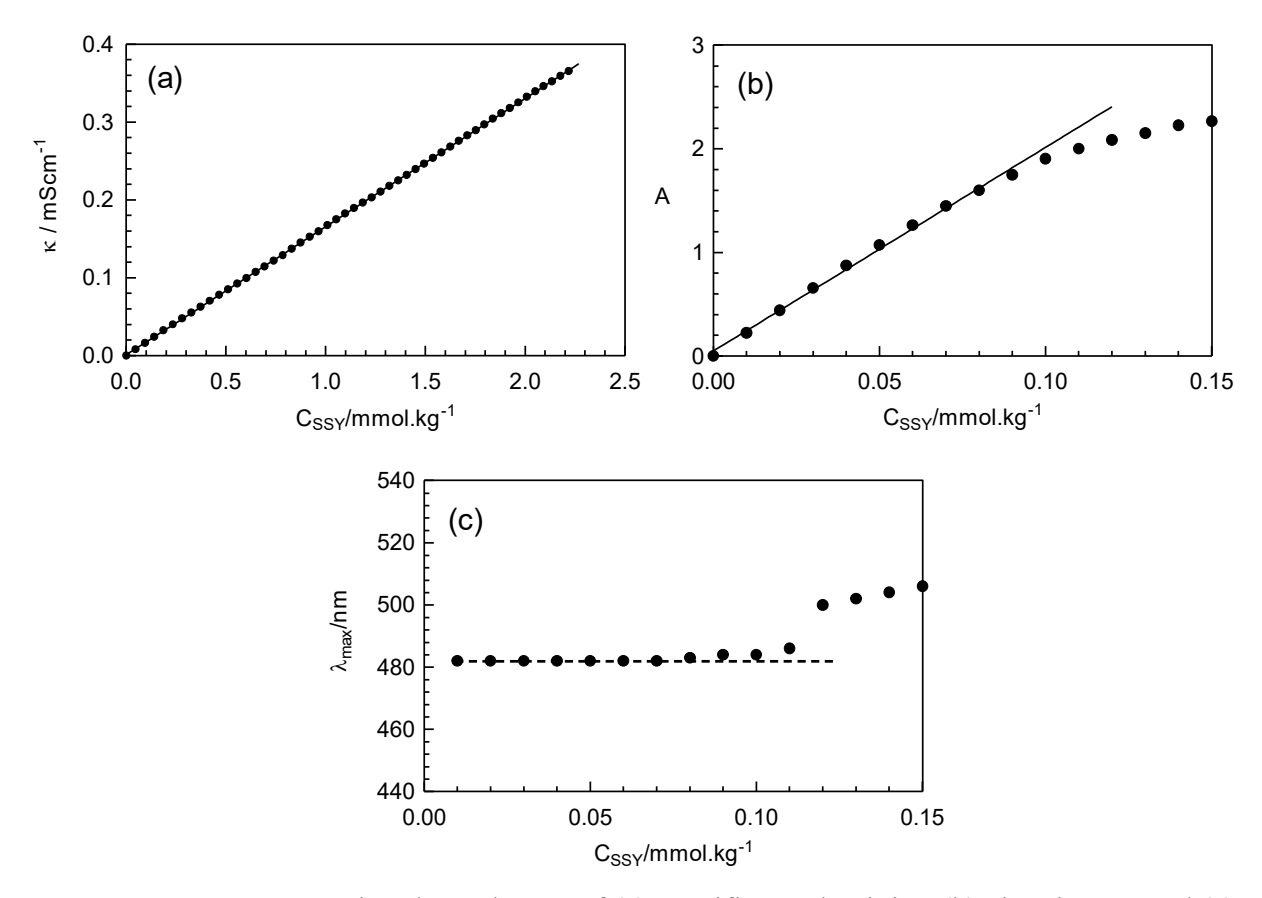


Figure 8. SSY concentration dependences of (a) specific conductivity, (b) absorbance, and (c) wavelength of maximum absorption in the concentration range of 0.00-2.21 mmol/kg at 25°C in the absence of DTMABr.

Now, let's investigate Figures 6 and 7 in details to find information on the aggregation behavior of SSY within the working concentration range, i.e. existing as monomer or higher-order aggregate in the absence of DTMABr. It is known that monomer SSY molecule has two absorption bands: a major one, which has a maximum around 480-482 nm, and a second one at \sim 314 nm [11,81,82]. While the major absorption band is related to the color of SSY due to the n- π * transition absorption of the chromophore groups of SSY molecule [82], the second one arises from the π - π * transition absorption related to the aromatic rings of SSY molecules [83,84]. For 0.04 mmol/kg, SSY exhibits characteristic UV-VIS absorption spectra given in the literature (Figure 9) [11]. Until the SSY-concentration reaches the concentration, at which the deviation from the Beer-Lambert's law starts (\sim 0.10 mmol/kg), similar spectra for $C_{\rm SSY}$ < 0.10 mmol/kg were recorded (Figure 6). However, at SSY concentrations greater than 0.10 mmol/kg,

three new bands can be seen: at 412 nm, 451 nm and 500 nm. There is no maximum wavelength shift for the band at 412 nm but its intensity increases as the concentration of SSY increases, especially $C_{SSY} > 0.296$ mmol/kg. The band at 451 nm shifts to 435 nm (blue shift) then to 445 nm (red shift) and the intensity of maximum absorption slightly increases within the chosen concentration range of SSY. The absorption band at 500 nm continuously shifts to higher wavelength (red shift) as a relatively broad peak. The main change in the UV-VIS spectra of the monomer SSY is observed around the major band. At low concentrations ($C_{SSY} < 0.10$ mmol/kg) the maximum absorption of major band is seen at 482 nm with no additional bands and the maximum absorption at 482 nm starts to disappear as the concentration of the SSY increases for C_{SSY}>0.10 mmol/kg (Figure 6). Especially, for C_{SSY} > 0.200 mmol/kg, no maximum absorption band at 482 nm was observed in the UV-VIS spectra. Because this band is related to the existence of SSY monomers in the solutions, at high SSY concentrations, this situation may be attributed to the absence of SSY as monomers in the solutions. To make a comprehensive interpretation of UV/VIS spectra of SSY solutions, we must consider two maximum absorption bands at 435 nm and 500 nm in the case of the disappearance of the band at 482 nm. At low SSY concentration, first, the intensity of the band at 482 nm decreases, and that at 500 nm increases with red shift. This situation continues until the band at 482 nm is disappeared. At the same time, the band at 435 nm shifts towards 445 nm. Note that the maximum absorption is observed in wavelengths greater than 500 nm (red shift). For further increase in the SSY concentration, now the band at 435 nm turned to be wavelength at which maximum absorption is observed with red shift. Consequently, in both cases, the shifts from 435 nm to 445 nm and from 500 nm to ~550 nm mean that the formation of J-aggregation of SSY is more probable for $C_{SSY} > 0.296$ mmol/kg. In other words, at low (high) surfactant concentrations, the SSY molecules form H-aggregates as shown in the literature (J-aggregates). This is in good aggreement with the conductivity results. Furthermore, the beginning of the

formation of J-aggregates after $C_{SSY} > 0.100$ mmol/kg is supported with the red shift in the λ_{max} values as a function of the increase in the SSY-concentration (Figure 8c).

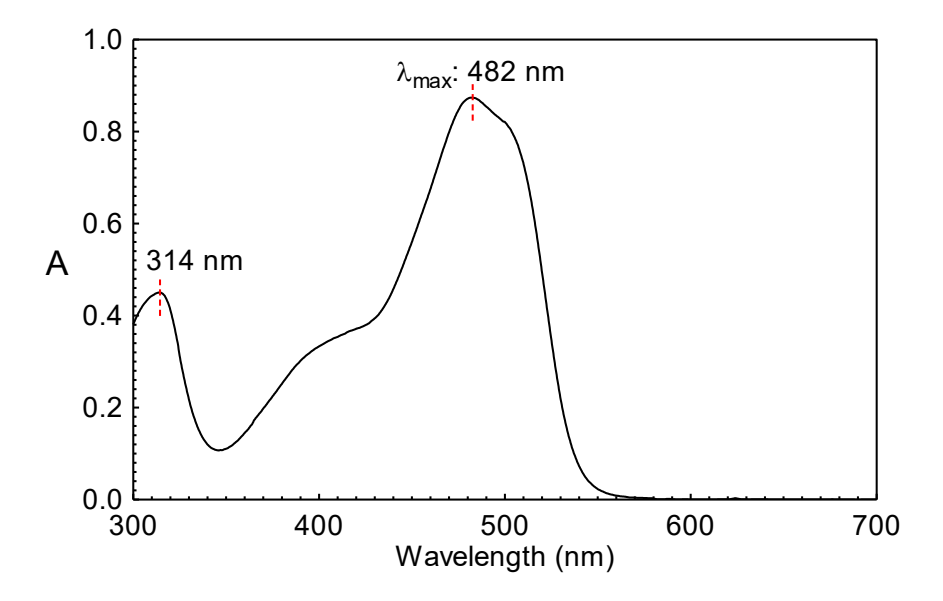


Figure 9. UV/VIS absorption spectrum of 0.04 mmol/kg SSY solution at 25°C in the absence of surfactant.

Figure 7 also include information about the aggregation-order of the SSY molecules in the absence of DTMABr. In a recent study, Fernandez-Perez and Marban analyzed the UV-VIS absorption spectra of methylene blue (MB) azo dye aggregation in water [85]. They studied the UV-VIS spectra of MB solutions for its large concentration range, 1.1x10⁻⁶ – 3.4x10⁻³ M, where the last concentration of MB is about 1.5 times greater than that of SSY used in the present study. The monomer MB gives a major band around 660 nm with a shoulder at 612 nm. As the concentration increases the absorption intensity of the band at 660 nm decreases while the maximum absorption is observed at 607 by shifting the wavelength of the band at 612, i.e. there exist two bands with a maximum at 607 nm which corresponds to the formation of dimer as a results of MB stackings. Further increase in the MB-concentration causes the disappearance of the band at 660 nm and shifting the maximum wavelength to 600 nm (blue shift) with relatively higher absorption intensity. The latter situation was attributed to the formation of tetramers of MB dyes. Almost similar results were obtained in our study (Figure 7). Thus, we can say that,

at the relatively low SSY concentrations > 0.10 mmol/kg, the dimer formation is observed and, approaching to 2.21x10⁻³ mol/kg SSY-concentration, the higher-order aggregate formation of SSY (tetramer or higher-order, considering the Ref. [85]) is more probable. Consequently, it can be concluded that while H-aggregates as dimers are formed at low SSY-concentrations, J-aggregate formations are favored as a higher-order at high SSY-concentrations. However, the formation of dye stacking as H-aggregate does not affect the conductivity of aqueous dye solutions with respect to that of dye molecules in a monomer state. The conductivity of SSY solutions exactly shows linear change with the concentration of SSY (Figure 8a). Thus, the gemini surfactant behavior of DTMABr/SSY obtained in the conductivity curves of DTMABr/SSY solutions (Figure 4 and 5) cannot not be attributed to the SSY stackings. Instead, it is clear that this behavior should be a result of surfactant/dye interactions.

After clarifying that SSY-stacking has no effect on the gemini surfactant behavior of DTMABr in the presence of SSY, we may proceed with discussing the analysis of conductivity results of aqueous DTMABr/SSY solutions as a function of SSY concentration in the solutions. Because the transition from monomer state to the micellar state gets more gradual around the cmc of DTMABr (Figure 4), Carpena' method, considering the Aguiar's approach, was applied to DTMABr/SSY solutions to evaluate their micellization parameters. For the calculations, C_C , C_1 , C_0 and C_4 are important but C_2 and C_3 not: the linear curves between C_C and C_1 in the premicellar region and above C_4 (post-micellar region) were used to find α and β values, and then $\Delta_{mic}G$. All values depending on SSY concentrations are given in Table 3. Furthermore, those values were plotted against SSY concentrations in Figures 10 and 11.

Table 3. SSY concentration dependence of micellization parameters of DTMABr at 25.0°C obtained from electrical conductivity measurements, considering the Carpena's method.

SSY/ mmol.kg ⁻¹	C _p / mmol.kg ⁻¹	C _C / mmol.kg ⁻¹	ΔC/ mmol.kg ⁻¹	C ₁ / mmol.kg ⁻¹	C _o / mmol.kg ⁻¹	C ₄ / mmol.kg ⁻¹	α	β	$\Delta_{ m mic}G/$ kj.mol ⁻¹
0.000			2.09	9.91	14.08	18.27	0.229	0.771	-36.33
0.040			1.93	9.83	14.15	18.47	0.231	0.769	-36.26
0.168	0.31	0.50	2.07	9.72	14.23	18.69	0.233	0.767	-36.20
0.296	0.29	0.75	2.34	9.64	14.38	19.02	0.237	0.763	-36.07
0.424	0.25	1.05	2.52	9.50	14.45	19.46	0.238	0.762	-36.03
0.553	0.22	1.17	2.57	9.41	14.56	19.70	0.242	0.758	-35.91
0.832	0.20	1.65	3.09	9.19	14.77	20.31	0.248	0.752	-35.73
1.11	0.18	2.12	3.36	8.88	15.09	21.44	0.252	0.748	-35.56
1.39	0.20	2.66	3.45	8.60	15.36	22.32	0.257	0.743	-35.38
1.66	0.18	3.13	3.64	8.31	15.57	22.85	0.265	0.735	-35.16
1.94	0.19	3.53	3.92	8.15	15.74	23.30	0.270	0.730	-35.01
2.21	0.17	3.79	4.21	7.97	16.01	24.23	0.277	0.723	-34.79

^a [55], ^b [56].

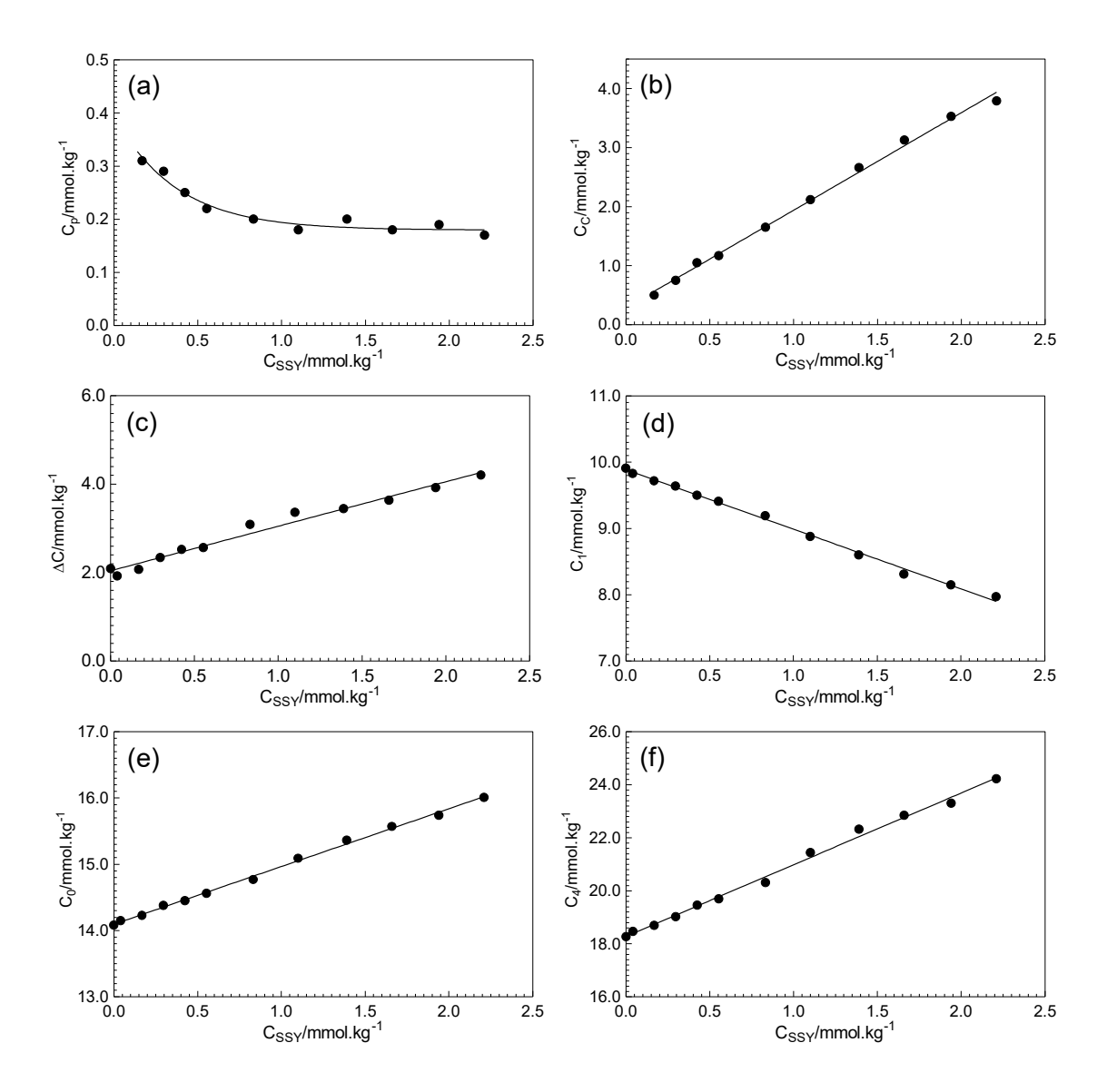


Figure 10. SSY concentration dependences of (a) C_p and (b) C_C from Williams's method, and (c) ΔC , (d) C_1 , (e) C_0 and (f) C_4 considering Carpena's method and Aguiar's approach.

By increasing the C_{SSY} , the C_1 values decrease (Figure 10d) and C_4 ones increase (Figure 10f), which indicates the increase in the concentration range ΔC (Figure 10c). Furthermore, the cmc of DTMABr is unfavored (Figure 10e) as supported by the change in β and $\Delta_{mic}G$. It is known that if the micellization is less favored the number of counterions bound to the surfactant head groups on the micelle surfaces decreases, i.e. smaller β (Figure 11b) or greater α (Figure 11a). Besides, the micellization Gibbs energy takes fewer negative values (Figure 11c).

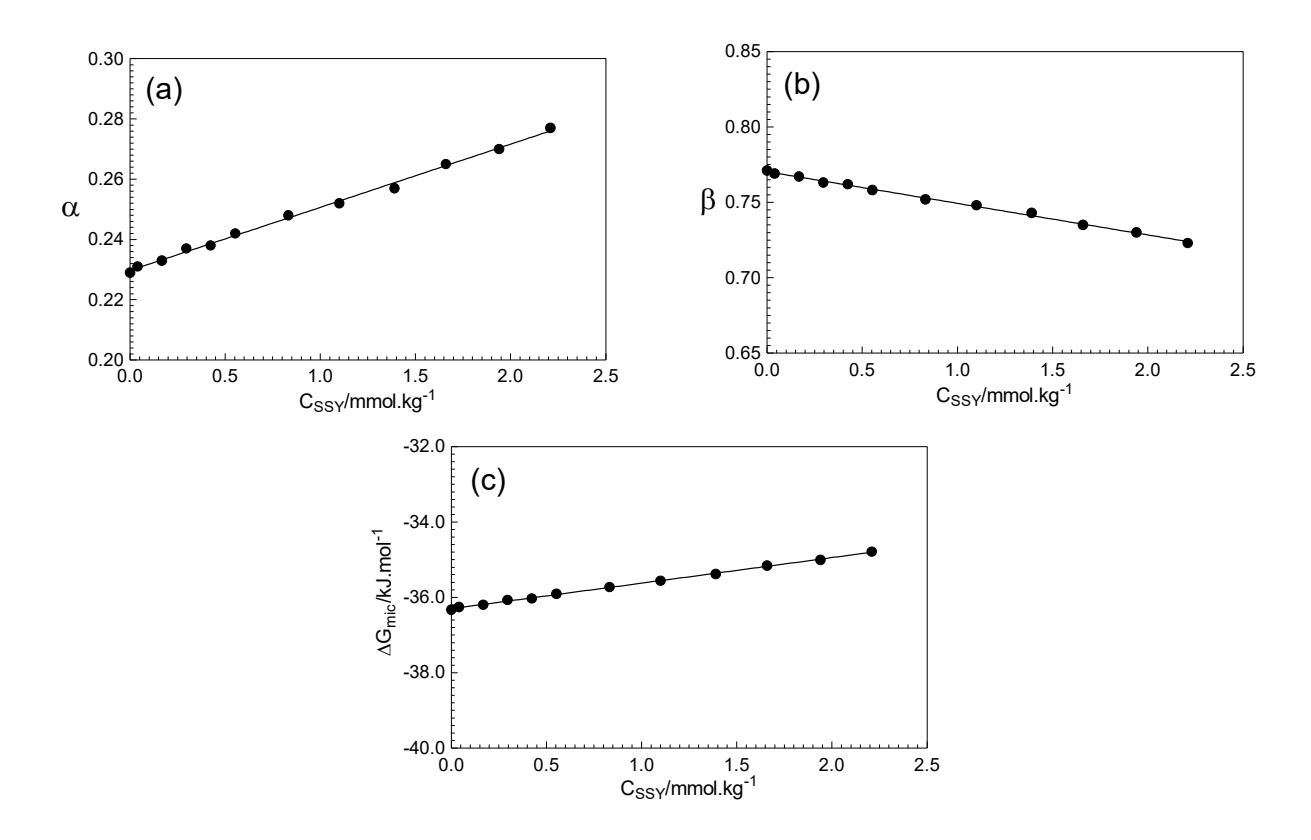


Figure 11. Changes in α , β and $\Delta_{mic}G$ as a function of SSY concentration in the solutions.

4. Conclusions

In the present study, we investigated the surfactant-dye interactions between cationic surfactant DTMABr and anionic azo dye Sunset Yellow. Differently from the existing studies on the aqueous DTMABr-SSY solutions in the literature, the properties of those solutions were studied at a relatively larger SSY concentration range. It was surprisingly observed that although DTMABr is a conventional single-chain surfactant, it exhibited gemini surfactant behavior at high SSY concentrations, as reported for tartrazine-gemini surfactant system, as a result of the surfactant-dye inetractions. For low SSY concentrations, that behavior was not observed which is in a good agreement with the literature. Furthermore, in the presence of DTMABr, the while SSY molecules at low concentrations stack in the form of H-aggregates at low SSY concentrations, the increase in its concentrations results in the formation of they show J-aggregation at high concentrationses. Consequently, tTo the best of our knowledge, this is the

first study which that shows both the gemini surfactant behavior of DTMABr in the presence of SSY and J-aggregations of SSY at high SSY concentrations in the presence of DTMABr. Considering the application of SSY in the cosmetic, food, etc., this study includes some useful merits.

Author contribution statement

Erol Akpinar, Antonio M. F. Neto and Oleg D. Lavrentovich designed the experimental parts of the studies, then analyzed and discussed the results. Nazli Uygur (NU) and Gokhan Topcu (GT) performed the experimental work. ODL research was supported by the U.S. National Science Foundation grant DMS-2106675.

Declaration of competing interest

The authors declare that they have no known competing financial interests or personal relationships that could have appeared to influence the work reported in this paper.

5. Acknowledgements

The authors thank the Scientific and Technological Research Council of Turkey (TÜBİTAK) [grant number: 217Z079]; Bolu Abant Izzet Baysal University Directorate of Research Projects Commission (BAP) [grant number: 2014.03.03.766] for supporting this work.

6. References

[1] Nurnberg E, Pohler W. Zur Kenntnis von 3-Komponenten-Mikroemulsionsgelen. In: Weiss A. (eds) Surfactants, Micelles, Microemulsions and Liquid Crystals. Progress in Colloid & Polymer Science, vol 69. Steinkopff; 1984.

- [2] Yang J. Interaction of surfactants and aminoindophenol dye. J Colloid Interface Sci 2004;274:237-43.
- [3] Ghoreishi SM, Nooshabadi M. Electromotive force studies about some dyes–cationic surfactants interactions in aqueous solutions. Dyes Pigm 2005;65:117-23.
- [4] Bagha ART, Bahrami H, Movassagh B, Arami M, Menger FM. Interactions of gemini cationic surfactants with anionic azo dyes and their inhibited effects on dyeability of cotton fabric. Dyes Pigm 2007;72:331-8.
- [5] Almeida MR, Stephani R, Dos Santos HF, Oliveira LFC. Spectroscopic and theoretical study of the "azo"-dye E124 in condensate phase: evidence of a dominant hydrazo form.

 J Phys Chem A 2010;114:526-34.
- [6] Nazar MF, Murtaza S. Physicochemical investigation and spectral properties of Sunset Yellow dye in cetyltrimethylammonium bromide micellar solution under different pH conditions. Color Technol 2014;130:191-9.
- [7] Simoncic B, Span J. A study of dye–surfactant interactions. Part 3. Thermodynamics of the association of C.I. Acid Orange 7 and cetylpyridinium chloride in aqueous solutions. Dyes Pigm 2000;46:1-8.
- [8] Chauan MS, Kumari N, Pathania S, Sharma K, Kumar G. A conductometric study of interactions between gelatin and sodium dodecyl sulfate (SDS) in aqueous-rich mixtures of dimethylsulfoxide. Colloids Surf A 2007;293:157-61.
- [9] Hossainzadeh R, Maleki R, Matin AA, Nikkhahi Y. Spectrophotometric study of anionic azo-dye light yellow (X6G) interaction with surfactants and its micellar solubilization in cationic surfactant micelles. Spectrochim Acta A 2008;69:1183-7.
- [10] Hashemi N, Sun G. Intermolecular Interactions between Surfactants and Cationic Dyes and Effect on Antimicrobial Properties. Ind Eng Chem Res 2010;49:8347-52.

- [11] Fazeli S, Sohrabi B, Tehrani-Bagha AR. The study of sunset yellow anionic dye interaction with gemini and conventional surfactants in aqueous solution. Dyes Pigm 2012;95:768-75.
- [12] Kartal E, Akbas H. Study on the interaction of anionic dye–nonionic surfactants in a mixture of anionic and nonionic surfactants by absorption spectroscopy. Dyes Pigm 2005;65:191-5.
- [13] Khan NM, Sarwar A. Study of dye–surfactant interaction: Aggregation and dissolution of yellowish in N-dodecylpyridinum chloride. Fluid Phase Equilib 2006;239:166-171.
- [14] Rafati AA, Azizian S, Chahardoli M. Conductometric studies of interaction between anionic dyes and cetylpyridinium bromide in water–alcohol mixed solvents. J Mol Liq 2008;137:80-7.
- [15] Ghoreishi SM, Behpour M, Nooshabadi MS. Interaction of Anionic Azo Dye and TTAB- Cationic Surfactant. J Braz Chem Soc 2009:20:460-5.
- [16] Sohrabi B, Bazyari A. Effect of ethylene glycol on micellization and surface properties of Gemini surfactant solutions. Colloid Surf A 2010:364;87-93.
- [17] Cheng X, Peng Y, Gao C, Yan Y, Huang J. Studying of 1-D assemblies in anionic azo dyes and cationic surfactants mixed systems. Colloid Surf A: Physicochem Eng Aspects 2013;422:10-8.
- [18] Simoncic B, Span J. A study of dye-surfactant interactions. Part 1. Effect of chemical structure of acid dyes and surfactants on the complex formation. Dyes Pigm 1998:36:1-14.
- [19] Minch MJ, Shah SS. Spectroscopic studies of hydrophobic association. Merocyanine dyes in cationic and anionic micelles. J Org Chem 1979;44:3252-5.
- [20] Moulik SP, Ghosh S, Das AR. Interaction of acridine orange monohydrochloride dye with sodiumdodecylsulfate, (SDS) cetyltrimethylammoniumbromide (CTAB) and p-tert-

- octylphenoxypolyoxy ethanol (Triton X 100) surfactants. Colloid Polym Sci 1979;257:645-55.
- [21] Nazar MF, Shah SS, Khosa MM. Interaction of azo dye with cationic surfactant under different pH conditions. J Surfact Deterg 2010;13:529-537.
- [22] Akpinar E, Topcu G, Reis D, Neto AMF. Effect of the anionic azo dye Sunset Yellow in lyotropic mixtures with uniaxial and biaxial nematic phases. J Mol Liq 2020;318:114010.
- [23] Akpinar E, Uygur N, Demir-Ordu O, Reis D, Neto AMF. Effect of the surfactant head-group size dependence of the dye-surfactant interactions on the lyotropic uniaxial to biaxial nematic phase transitions. J Mol Liq 2021;332:115842.
- [24] Shahir AA, Javadian S, Razavizadeh M, Gharibi H. Comprehensive study of tartrazine/cationic surfactant interaction. J Phys Chem B 2011;115:14435-44.
- [25] Ali A, Alam M, Farooq U, Uzair S. Effect of the nature of counterion on the micellar properties of cationic surfactants: a conductometric study. Phys Chem Liq 2018;56:528-43.
- [26] Streubel S, Schulze-Zachau F, Weissenborn E, Braunschweig B. Ion pairing and adsorption of azo dye/C16TAB surfactants at the air—water interface. J Phys Chem C Nanomater Interface 2017;121:27992-8000.
- [27] Esan OS. Temperature dependence on the molecular interaction of amaranth dye with cetyltrimethylammonium bromide in the premicelle region: A spectroscopy study. Chem Sci Eng Res 2020;2:21-6.
- [28] Karukstis KK, Savin DA, Loftus CT, Angelo NDD. Spectroscopic studies of the interaction of methyl orange with cationic alkyltrimethylammonium bromide surfactants J Colloid Interface Sci 1998;203:157–63.

- [29] Petcu AR, Rogozea EA, Lazar CA, Olteanu NL, Meghea A, Mihaly M. Specific interactions within micelle microenvironment in different charged dye/surfactant systems. Arab J Chem 2016;9:9-17.
- [30] Ghosh S, Mondal S, Das S, Biswas R. Spectroscopic investigation of interaction between crystal violet and various surfactants (cationic, anionic, nonionic and gemini) in aqueous solution. Fluid Phase Equilib 2012;332:1-6.
- [31] Alavijeh MR, Javadian S, Gharibi H, Moradi M, Bagha ART, Shahir AA. Intermolecular interactions between a dye and cationic surfactants: Effects of alkyl chain, head group, and counterion. Colloids Surf A: Physicochem Eng Aspects 2011;380:119-27.
- [32] Abe M, Kasuya T, Ogino K. Thermodynamics of surfactant-dye complex formation in aqueous solutions. Sodium alkyl sulfates and azo oil dye systems. Colloid Polym Sci 1988;266:156–63.
- [33] Ain Q, Khurshid S, Gul Z, Khatoon J, Shah MR, Hamid I, Khan IAT, Aslam F. RSC Advances, 10 (2020) 1021-41.
- [34] Abe M, Ohsato M, Ogino K. Interaction between anionic surfactants and oil dye in the aqueous solutions. IV. The effect of alkyl chain length in surfactant molecule on the protonation equilibrium of azo dye. Colloid Polym Sci 1984;262:657–61.
- [35] Tajalli H, Gilani AG, Zakerhamidi MS, Moghadam M. Effects of surfactants on the molecular aggregation of rhodamine dyes in aqueous solutions. Spectrochim Acta A: Mol Biomol Spect 2009;72:697-702.
- [36] Würthner F, Kaiser TE, Saha-Möller CR. J-Aggregates: From serendipitous discovery to supramolecular engineering of functional dye materials. Angew Chem Int Ed 2011;50:3376-410.
- [37] Zhang L, Cole JM. Dye aggregation in dye-sensitized solar cells. J Mater Chem A 2017;5:19541-59.

- [38] Bricks JL, Slominskii YL, Panas ID, Demchenko AP. Fluorescent J-aggregates of cyanine dyes: basic research and applications review. Methods Appl Fluoresc 2018;6:012001.
- [39] Diaz-Garcia ME, Sanz-Medel A. Dye-surfactant interactions: a review. Talanta 1986;33:255-64.
- [40] Garcia-Rio L, Hervella P, Mejuto JC, Parajo M. Spectroscopic and kinetic investigation of the interaction between crystal violet and sodium dodecylsulfate. Chem Phys 2007;335:164-76.
- [41] Lydon J. Chromonic review. J Mater Chem 2010;20:10071–99.
- [42] Berejnov VV, Cabuil V, Perzynski R, Raikher YL, Lysenko SN, Sdobnov VN. Lyotropic nematogenic system potassium laurate/1-decanol/water: method of synthesis and study of phase diagrams. Cryst Rep 2000;45(3):493-500.
- [43] Akpinar E, Otluoglu K, Turkmen M, Canioz C, Reis D, Neto AMF. Effect of the presence of strong and weak electrolytes on the existence of uniaxial and biaxial nematic phases in lyotropic mixtures Liq. Cryst. 2016;43:1693-708.
- [44] Horowitz VR, Janowitz LA, Modic AL, Heiney PA, Collings PJ. Aggregation behavior and chromonic liquid crystal properties of an anionic monoazo dye. Phys Rev E 2005;72:041710.
- [45] Park H, Kang S, Tortora L, Nastishin Y, Finotello D, Kumar S, Lavrentovich OD. Self-assembly of lyotropic chromonic liquid crystal sunset yellow and effects of ionic additives. J Phys Chem B 2008;112:16307-19.
- [46] Williams RJ, Philips JN, Mysels KJ. The critical micelle concentration of sodium lauryl sulphate at 25°C. Trans Faraday Soc 1955;51:728–37.

- [47] Pérez-Rodríguez M, Prieto G, Rega C, Varela LM, Sarmiento F, Mosquera, V. A comparative study of the determination of the critical micelle concentration by conductivity and dielectric constant measurements. Langmuir 1998;14:4422-6.
- [48] Carpena P, Aguiar J, Bernaola-Galvan P, Ruiz CC. Problems associated with the treatment of conductivity-concentration data in surfactant solutions: Simulations and experiments. Langmuir 2002;18:6054-8.
- [49] Koya PA, Wagay TA, Ismail K. Conductometric studies on micellization of cationic surfactants in the presence of glycine. J Sol Chem 2015;44:100-11.
- [50] Zheng P, Cai D, Qiao K, Zhao J, Shen W. Temperature dependence of micellization behavior of N',N'-didodecyl-N,N,N',N'-tetramethylhexane-1,6-diammonim dibromide and 1-dodecyl-3-methylimidazolium bromide in aqueous solutions. J Mol Liq 2020;308:112999.
- [51] Musale SP, Babalsure PS, Pawar DD. Volumetric properties, viscosity coefficients and aggregation behaviour of DBU-acetate protic ionic liquid in molecular solvents. J Mol Liq 2020;319:114917.
- [52] Chaudhary NK, Bhattarai A, Guragain B, Bhattarai A. Conductivity, surface tension, and comparative antibacterial efficacy study of different brands of soaps of Nepal. J Chem 2020;6989312:1-13.
- [53] Aguiar J, Carpena P, Molina-Bolivar JA, Ruiz CC. On the determination of the critical micelle concentration by the pyrene 1:3 ratio method. J Colloid Interface Sci 2003;258:116-22.
- [54] Sugihara G, Nakano T, Sulthana SB, Rakshit AK. Enthalpy-entropy compensation rule and compensation temperature observed in micelle formation of different surfactants in water. What is the so-called compensation temperature? J Oleo Sci 2001;50:29-39.
- [55] Rosen MJ. Surfactants and Interfacial Phenomena. 2nd edition. New York: Wiley; 1989.

- [56] Fenta AD. Surface and thermodynamic studies of micellization of surfactants in binary mixtures of 1,2-ethanediol and 1,2,3-propanetriol with water. Int J Phys Sci 2015;10:276-88.
- [57] Ghosh S, Moulik SP. Interfacial and micellization behaviors of binary and ternary mixtures of amphiphiles (Tween-20, Brij-35, and sodium dodecyl sulfate) in aqueous medium. J Colloid Interface Sci 1998;208:357-66.
- [58] Oremusova J, Vitkova Z, Vitko A, Tarnik M, Miklovicova E, Ivankova O, Murgas J, Krchnak D. Effect of molecular composition of head group and temperature on micellar properties of ionic surfactants with C12 alkyl chain. Molecules 2014;24;651 (1-21).
- [59] Mahbub S, Rahman M, Rana S, Rub MA, Hoque MA, Khan MA, Asiri AM. Aggregation behavior of sodium dodecyl sulfate and cetyltrimethylammonium bromide mixtures in aqueous/chitosan solution at various temperatures: An experimental and theoretical approach. J Surf Deterg 2019;22:137-52.
- [60] Kale KM, Zana R. Effect of the nature of the counterion on the volume change upon micellization of ionic detergents in aqueous solutions. J Colloid Interface Sci 1977;61:312-22.
- [61] Mehta SK, Bhasim KK, Chauhan R, Dham S. Effect of temperature on critical micelle concentration and thermodynamic behavior of dodecyldimethylethylammonium bromide and dodecyltrimethylammonium chloride in aqueous media. Colloid Surf A 2005;255:153-7.
- [62] Fisicaro E, Biemmi M, Compari C, Duce E, Peroni M. Thermodynamics of aqueous solutions of dodecyldimethylethylammonium bromide. J Colloid Interface Sci 2007;305:301-7.

- [63] Junquera E, Aicart E. Mixed micellization of dodcylethyldimethylammonium bromide and dodecyltrimethylammonium bromide in aqueous solution. Langmuir 2002;18:9250-8.
- [64] Bales BL, Zana R. Characterization of micelles of quaternary ammonium surfactants as reaction media I: Dodeclytrimethylammonium bromide and chloride. J Phys Chem B 2002;106:1926-39.
- [65] Malliaris A, Le Moigne J, Sturm J, Zana R. Temperature dependence of the micelle aggregation number and rate of intramicellar excimer formation in aqueous surfactant solutions. J Phys Chem 1985;89:2709–13.
- [66] Šarac B, Bešter-Rogač M. Temperature and salt-induced micellization of dodecyltrimethylammonium chloride in aqueous solution: A thermodynamic study. J Colloid Interface Sci 2009;338:216-21.
- [67] Bach J, Blandamer MJ, Burgess J, Cullis PM, Soldi LG, Bijma K, Engberts JPFN, Kooreman PA, Kacperska A, Chowdoji K, Subha MCS. Titration calorimetric and spectrophotometric studies of micelle formation by alkyltrimethylammonium bromide in aqueous solution. J Chem Soc Fraday Trans 1995;91:1229-35.
- [68] Zielinski R, Ikeda S, Nomura H, Kato S. Effect of temperature on micelle formation in aqueous solutions of alkyltrimethylammonium bromides. J Colloid Interface Sci 1989;129:175-84.
- [69] Lopez-Fontan JL, Suarez MJ, Mosquera V, Sarmiento F. Mixed micelles of n-alkyltrimethylammonium bromides: influence of alkyl chain length. Phys Chem Chem Phys. 1999;1:3583-87.
- [70] Ghasemi A, Bagheri A. Effects of alkyl chain length on synergetic interaction and micelle formation between a homologous series of n-alkyltrimethylammonium bromides and amphiphilic drug propranolol hydrochloride. J Mol Liq 2020;298:111948.

- [71] Jaber R, Wasbrough MJ, Holdaway JA, Adler KJ. Interactions between quaternary ammonium surfactants and polyethylenimine at high pH in film forming systems. J Colloid Interface Sci 2015;449:286-96.
- [72] Kalyanasundram K. Photochemistry im Microheterogeneous Systems. New York: Academic Press; 1987.
- [73] Ruiz CC. A photophysical study of micellization of cetyltrimethylammonium bromide in urea-water binary mixtures. Mol Phys 1995;86:535-46.
- [74] Peyre V, Bouguerra S, Testard F. Micellization of dodecyltrimethylammonium bromide in water-dimethylsulfoxide mixtures: A multi-length scale approach in a model system. J Colloid Interface Sci 2013;389:164-74.
- [75] Chauhan S, Kaur M, Kumar K, Chauhan MS. Study of the effect of electrolyte and temperature on the critical micelle concentration of dodecyltrimethylammonium bromide in aqueous medium. J Chem Thermodynamics 2014;78:175-81.
- [76] Aguiar J, Molina-Bolivar JA, Peula-Garcia JM, Ruiz CC. Thermodynamics and micellar properties of tetradecyltrimethylammonium bromide in formamide—water mixtures. J Colloid Interface Sci 2002;255:382–90.
- [77] Edwards DJ, Jones JW, Lozman O, Ormerod AP, Sintyureva M, Tiddy GJT. Chromonic liquid crystal formation by edicol Sunset Yellow. J Phys Chem B 2008;112:14628–36.
- [78] Muhammad MT, Khan MN. Oppositely charged dye surfactant interactions: Extent and selectivity of ion pair formation. J Mol Liq 2018;266:591-6.
- [79] Navarro A, Sanz F. Dye aggregation in solution: study of C.I. direct red I. Dyes Pigm 1999;40:131-9.
- [80] Behera GB, Behera PK, Mishra BK. Cyanine dyes: self aggregation and behaviour in surfactants a review. J Surf Sci Technol 2007;23:1-31.

- [81] Wang Y, Zhang Z, Xiao Y, Li N. Spectrophotometric determination of Sunset Yellow in beverage after preconcentration by the cloud point extraction method. Analy Methods 2014;6:8901-5.
- [82] Nascimento GE, Cavalcanti VOM, Santana RMR, Sales DCS, Rodríguez-Díaz JM, Napoleão DC, Duarte MMMB. Degradation of a Sunset Yellow and Tartrazine dye mixture: Optimization using statistical design and empirical mathematical modeling", Water Air Soil Pollut 2020;231:254 (1-17).
- [83] Oancea, P, Meltzer V. Photo-Fenton process for the degradation of tartrazine (E102) in aqueous medium. J Taiwan Inst Chem Eng 2013;44:990–4.
- [84] Ghoneim MM, El-Desoky HS, Zidan NM. Electro-Fenton oxidation of sunset yellow FCF azo-dye in aqueous solutions. Desalination 2011;274:22–30.
- [85] Fernandez-Perez A, Marban G. Visible light spectroscopic analysis of methylene blue in water; What comes after dimer?. ACS Omega 2020;5:29801-15.